

Effect of stoichiometry on the dielectric properties and soft mode behavior of strained epitaxial SrTiO₃ thin films on DyScO₃ substrates

Che-Hui Lee, Volodymyr Skoromets, Michael D. Biegalski, Shiming Lei, Ryan Haislmaier, Margitta Bernhagen, Reinhard Uecker, Xiaoxing Xi, Venkatraman Gopalan, Xavier Martí, Stanislav Kamba, Petr Kužel, and Darrell G. Schlom

Citation: *Applied Physics Letters* **102**, 082905 (2013); doi: 10.1063/1.4793649

View online: <http://dx.doi.org/10.1063/1.4793649>

View Table of Contents: <http://scitation.aip.org/content/aip/journal/apl/102/8?ver=pdfcov>

Published by the [AIP Publishing](#)

Articles you may be interested in

[Compositional engineering of BaTiO₃/\(Ba,Sr\)TiO₃ ferroelectric superlattices](#)

J. Appl. Phys. **114**, 104102 (2013); 10.1063/1.4820576

[Enhanced microwave dielectric tunability of Ba_{0.5}Sr_{0.5}TiO₃ thin films grown with reduced strain on DyScO₃ substrates by three-step technique](#)

J. Appl. Phys. **113**, 044108 (2013); 10.1063/1.4789008

[Soft mode behavior in SrTiO₃ / DyScO₃ thin films: Evidence of ferroelectric and antiferrodistortive phase transitions](#)

Appl. Phys. Lett. **95**, 232902 (2009); 10.1063/1.3271179

[Crystal structure and electrical property comparisons of epitaxial Pb \(Zr , Ti \) O₃ thick films grown on \(100 \) CaF₂ and \(100 \) SrTiO₃ substrates](#)

J. Appl. Phys. **105**, 061614 (2009); 10.1063/1.3073823

[Relaxor ferroelectricity in strained epitaxial Sr Ti O₃ thin films on Dy Sc O₃ substrates](#)

Appl. Phys. Lett. **88**, 192907 (2006); 10.1063/1.2198088

Want to publish your paper in the
#1 MOST CITED journal in applied physics?

With *Applied Physics Letters*, you can.

AIP | Applied Physics
Letters

THERE'S POWER IN NUMBERS. Reach the world with AIP Publishing.



Effect of stoichiometry on the dielectric properties and soft mode behavior of strained epitaxial SrTiO₃ thin films on DyScO₃ substrates

Che-Hui Lee,^{1,2} Volodymyr Skoromets,³ Michael D. Biegalski,⁴ Shiming Lei,² Ryan Haislmaier,² Margitta Bernhagen,⁵ Reinhard Uecker,⁵ Xiaoxing Xi,⁶ Venkatraman Gopalan,² Xavier Martí,^{3,7} Stanislav Kamba,³ Petr Kuzel,³ and Darrell G. Schlom^{1,8,a)}

¹Department of Materials Science and Engineering, Cornell University, Ithaca, New York 14853, USA

²Department of Materials Science and Engineering, Pennsylvania State University, University Park, Pennsylvania 16802, USA

³Institute of Physics, ASCR, Na Slovance 2, 182 21 Prague 8, Czech Republic

⁴Center for Nanophase Materials Sciences, Oak Ridge National Laboratory, Oak Ridge, Tennessee 37831, USA

⁵Leibniz Institute for Crystal Growth, Max-Born-Straße 2, D-12489 Berlin, Germany

⁶Department of Physics, Temple University, Philadelphia, Pennsylvania 19122, USA

⁷Department of Physics, Faculty of Mathematics and Physics, Charles University, Prague, Czech Republic

⁸Kavli Institute at Cornell for Nanoscale Science, Ithaca, New York 14853, USA

(Received 3 December 2012; accepted 12 February 2013; published online 1 March 2013)

The effect of stoichiometry on the dielectric properties and soft mode behavior of strained epitaxial Sr_{1+x}TiO_{3+δ} films grown on DyScO₃ substrates is reported. Direct comparisons between nominally stoichiometric and non-stoichiometric films have been performed through measurements of lattice parameters, temperature-dependent permittivities, second harmonic generation, and terahertz dielectric spectra. The nominally stoichiometric film shows dispersion-free low-frequency permittivity with a sharp maximum and pronounced soft mode behavior. Our results suggest that strained perfectly stoichiometric SrTiO₃ films should not show relaxor behavior and that relaxor behavior emerges from defect dipoles that arise from non-stoichiometry in the highly polarizable strained SrTiO₃ matrix.

© 2013 American Institute of Physics. [<http://dx.doi.org/10.1063/1.4793649>]

Pure bulk SrTiO₃ is a quantum paraelectric material at low temperatures where zero-point motion of the titanium ions suppresses the ferroelectric transition,¹ leading to so-called incipient ferroelectric behavior.² The static dielectric constant of single crystalline SrTiO₃ is around 300 at room temperature and rapidly increases upon cooling, saturating at near 24 000 at 4 K.¹ This delicate quantum paraelectric state can be easily upset by small perturbations such as impurity doping,^{3,4} oxygen isotope substitution,⁵ electric field,^{6,7} and mechanical stress.⁸ Biaxial tensile strain has been used to induce room-temperature ferroelectricity in SrTiO₃ thin films;⁹ however, the dielectric constant and loss of such strained films were found to depend on frequency in a way consistent with them being relaxor ferroelectrics.^{10,11}

Although relaxor behavior was unexpected, it was proposed that all SrTiO₃ films and bulk crystals are relaxor ferroelectrics.¹² The origin of the relaxor behavior was attributed to pre-existing polar nanoregions originating from unintentional strontium non-stoichiometry in nominally stoichiometric samples.¹² If this hypothesis is correct, precise composition control is critical to obtain the intrinsic and desirable properties of SrTiO₃ in both bulk and thin film forms, e.g., high dielectric permittivity, low dielectric loss, low leakage current, low fatigue, and dispersion-free permittivity.

In this letter, we investigate the effect of stoichiometry on the dielectric properties and soft mode behavior of strained epitaxial Sr_{1+x}TiO_{3+δ} (−0.05 < x < 0.05) films. The

films are grown on DyScO₃ substrates, the same system in which relaxor ferroelectricity in the vicinity of room temperature was observed.^{9–11} Although precise stoichiometry is difficult to measure in thin films, the dielectric properties were observed to change noticeably in the vicinity of stoichiometric SrTiO₃. Films that were measurably off in stoichiometry (either strontium-rich or strontium-poor) showed relaxor ferroelectric behavior. In contrast, a predominantly displacive ferroelectric phase transition (and what we believe to be the intrinsic properties of strained SrTiO₃) was observed in nominally stoichiometric films, i.e., films with no detectable deviation from stoichiometric by our measurement methods.

50 nm thick Sr_{1+x}TiO_{3+δ} films were grown on well-oriented (±0.1°) (110) DyScO₃ substrates by codeposition from strontium, titanium, and O₂ + ~10% O₃ molecular beams in a Veeco GEN10 oxide molecular-beam epitaxy (MBE) system. The oxidant background pressure (O₂ + ~10% O₃) was maintained at 5 × 10^{−7} Torr during and after growth until the sample cooled below 200 °C to minimize oxygen vacancies. The substrate temperature, measured by an optical pyrometer, was held at 700 °C during growth. Additional details on film growth and *in situ* calibration are given in Supplementary Fig. S1 of Ref. 13. The (110) DyScO₃ substrate has an average in-plane pseudocubic lattice constant of ~3.949 Å at room temperature,¹⁴ about 1% larger than SrTiO₃. This allows for the growth of thin coherently strained SrTiO₃ films, in which the ferroelectric phase is stabilized by biaxial tensile strain and the transition temperature is promoted to the vicinity of room temperature.⁹

^{a)}Electronic mail: schlom@cornell.edu.

The surface reconstruction of a strontium-rich (001) SrTiO₃ surface is characterized by a half-order diffraction streak between the 00 and 10 spots of the zeroth order Laue zone along the SrTiO₃ [110] azimuth, while a titanium-rich surface shows half-order streaks along the [100] and [210] azimuths.^{15–17} Sr:Ti = 1:1 fluxes were achieved by fine tuning the strontium source temperature during the deposition of SrTiO₃ until no surface reconstructions were observed along the [100], [110], or [210] azimuths of the growing SrTiO₃ film. Regular and persistent reflection high-energy electron diffraction (RHEED) intensity oscillations, which indicate changes in surface step density,¹⁸ of the 10 spot along the [110] azimuth were observed. The time needed for the growth of one unit cell of SrTiO₃ was calculated from the period of the oscillation and used for the growths that followed.

To grow SrTiO₃ films as stoichiometric as possible, the strontium-rich and titanium-rich half-order reconstruction features were monitored and compensated for with intermittent closing of the Sr/Ti shutter when infrequently needed, while the strontium source temperature and Ti-BallTM,¹⁹ current were held constant. Real-time RHEED monitoring and infrequent selective flux interruption effectively controlled the cation stoichiometry by compensating for the slow drift of the flux of each source and enabled the growth of nominally stoichiometric SrTiO₃ films. For the off-stoichiometric samples, the temperature of the strontium effusion cell was changed according to calibration performed with a quartz crystal microbalance (QCM) prior to the growths to achieve the desired atomic fluxes and no flux interruption was performed; the RHEED patterns indicated that the films were off composition throughout film growth.

The film structure, including out-of-plane and in-plane lattice constants and crystallinity, was examined by four-circle x-ray diffraction (XRD) using Cu K α ₁ radiation on a high-resolution Philips X'Pert Pro MRD diffractometer with a hybrid monochromator on the incident side and a triple axis/rocking curve attachment on the diffracted side. The out-of-plane lattice constants of the Sr_{1+x}TiO_{3+ δ} ($-0.05 < x < 0.15$) films were calculated from the 00 l film peak positions in the θ -2 θ scans²⁰ and are plotted as a function of strontium content in Fig. 1. The nominally stoichiometric sample has the smallest out-of-plane spacing, 3.8802 ± 0.0003 Å. The out-of-plane lattice constant of a commensurate SrTiO₃ film on (110) DyScO₃ calculated using the temperature dependent elastic constants of bulk SrTiO₃ (Ref. 21) is 3.8783 ± 0.0015 Å. As the results in Fig. 1 show, for non-stoichiometric films, this value increases independent of whether the film is strontium or titanium rich. This trend of lattice expansion is in agreement with previous findings for homoepitaxial SrTiO₃ films grown by MBE²² and illustrates that the out-of-plane lattice constant can be used to establish that the SrTiO₃ films are within about $\pm 1\%$ of stoichiometric. The slightly larger out-of-plane lattice constant (3.8833 ± 0.0005 Å) of SrTiO₃/DyScO₃ found by Biegalski *et al.*¹⁰ imply that the relaxor behavior reported in Ref. 10 likely originated from a small ($\sim 3\%$) off-stoichiometry in the samples studied. Slight non-stoichiometry would also explain the variation in the out-of-plane lattice spacing observed in Ref. 23 for commensurate

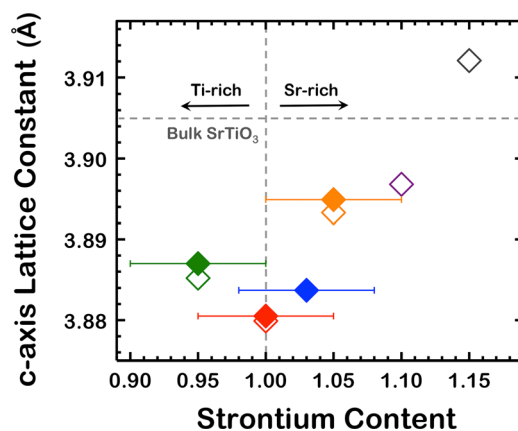


FIG. 1. Out-of-plane lattice constant as a function of strontium excess in Sr_{1+x}TiO_{3+ δ} ($-0.05 < x < 0.15$) films grown on (110) DyScO₃ substrates. Dashed lines indicate the lattice spacing and stoichiometry of bulk SrTiO₃. Both solid and open diamonds are data points. The error bar of lattice constants is about the size of the symbols, while the error bar of the strontium content determined from RBS measurements are $\sim 5\%$. Measurements performed on selected samples (solid symbols) are shown in Figs. 2–4, S1, S2, and S3.

SrTiO₃/DyScO₃ films, which also exhibited relaxor behavior. The in-plane lattice constants and crystalline quality were also assessed and are shown in Supplementary Fig. S1 of Ref. 13.

The composition of selected films (solid symbols in Fig. 1) was verified by Rutherford backscattering spectrometry (RBS); those films were within experimental error ($\pm 5\%$ for our RBS measurements) of the expected compositions based on shutter time adjustments (see Supplementary Fig. S2 of Ref. 13).

The dielectric properties of selected films were measured using Cr/Au interdigitated electrodes deposited on top of the films. Dielectric permittivity and loss tangent ($\tan \delta$), see Fig. 2, were measured over the temperature range of 10–350 K from

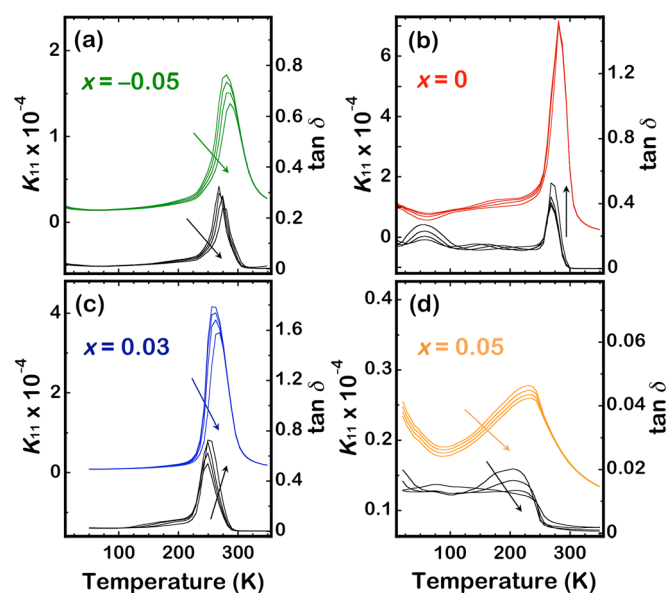


FIG. 2. In-plane dielectric constant (K_{11} , curves in color) and $\tan \delta$ (curves in black) as a function of temperature of the Sr_{1+x}TiO_{3+ δ} films grown on (110) DyScO₃ substrates with (a) $x = -0.05$, (b) $x = 0$, (c) $x = 0.03$, and (d) $x = 0.05$. Arrows indicate the direction of shift of the measured data with increasing measurement frequency in the sequence 1, 10, 100, and 1000 kHz.

1 kHz to 1 MHz using an Agilent E4980A high precision LCR meter with a Lake Shore 332 temperature controller. The in-plane dielectric constant (K_{11}) was calculated using a partial capacitance approach.²⁴ The peak value ($K_{11,max}$) $\sim 70\,000$ at 280 K of the $x=0$ nominally stoichiometric sample is much higher than those of the $x=-0.05$ and $x=0.03$ off-stoichiometric samples. In addition, the temperature of the permittivity maximum (T_{max}) of the $x=-0.05$ and $x=0.03$ samples are ~ 280 K and ~ 265 K, respectively, and frequency dependent, while T_c of the $x=0$ sample is ~ 280 K without frequency dispersion. The paraelectric-to-ferroelectric transition temperature (T_c) of the nominally stoichiometric sample is in agreement with the predicted transition temperature from thermodynamic analysis.²⁵

The ferroelectric transition in SrTiO₃ is driven by the soft mode, the transverse optical phonon with the lowest frequency. According to lattice dynamical theory and the Lyddane-Sachs-Teller relation, the dielectric permittivity is inversely proportional to the square of the soft mode frequency.²⁶ Therefore, the degraded permittivity in the off-stoichiometric SrTiO₃ sample could be attributed to the defect-sensitive soft mode behavior in the film (discussed below). The structural disorder coming from the insertion of extra SrO monolayers at random positions along {100} SrTiO₃ planes (i.e., Ruddlesden-Popper defects²⁷) that shift and terminate continuous Ti–O–Ti chains between TiO₆ octahedra could be responsible for the lower observed $K_{11,max}$ and T_{max} . The structural relaxation in strontium-rich samples is also a reason for the lower T_{max} .

The presence of frequency dispersion in the vicinity of the $K_{11}(T)$ peak is a universal signature of relaxor ferroelectrics. Compositional disorder and related random electric fields are believed to cause the relaxor behavior of mixed ABO₃ perovskite oxides such as Pb(Mg_{1/3}Nb_{2/3})O₃ and La-doped PbZr_{1-x}Ti_xO₃.²⁸ Relaxor behavior can also be induced by introducing impurities into an incipient ferroelectric (e.g., Ca-doped KTa_{1-x}Nb_xO₃,²⁹ Ca- and Bi-doped SrTiO₃^{3,4}), or into a ferroelectric (e.g., Ce-doped BaTiO₃³⁰). Point defects, including impurity-oxygen vacancy clusters or anti-site defects, can lead to the formation of dipolar entities which polarize a small volume around them and form polar nanoregions.²⁸ These polar nanoregions can be reduced in number by decreasing the point defect concentration as occurs as the SrTiO₃ films get closer to being stoichiometric; such improvement would lead to a flattening of the permittivity dispersion at low frequencies [Fig. 2(b)].

It is worthy to note that the frequency dependence of $\tan \delta$ behaves differently in the films with $x=-0.05$ and $x=0.05$ (Figs. 2(a) and 2(d)) than it does for the films with $x=0$ and $x=0.03$ (Figs. 2(b) and 2(c)). For more stoichiometric films, the maximum in $\tan \delta$ increases with increasing measurement frequency. This is typical of a broad relaxation, which either slows down or broadens towards lower frequencies with decreasing temperature.³¹ The opposite trend is observed for samples with $x=-0.05$ and $x=0.05$, i.e., for samples with a higher concentration of point defects. The observed behavior may stem from the presence of a second low-frequency relaxation with the mean relaxation frequency below the spectral range of our measurement, which slows down during cooling. Such relaxation can be attributed to defects.

The onset of the absence of inversion symmetry was probed optically by second harmonic generation (SHG). SHG signal as a function of temperature of selected films (solid symbols in Fig. 1) was measured on cooling and heating (Fig. 3). No SHG signal was observed from the bare DyScO₃ substrate indicating that the changes in the SHG signal only came from the Sr_{1+x}TiO_{3+ δ} thin films. In order to make a relative comparison between different samples, the incident laser power was kept constant. Table I summarizes the T_{max} measured at 1 kHz and the onset temperature of the SHG signal (T_{SHG}) measured on cooling and heating. While cooling through T_{SHG} , polar nanoregions start to nucleate and the center of symmetry is locally broken in the film. Such behavior is usually observed in relaxor materials at their Burns temperature.²⁸ Polar nanoregions have, however, also been observed above T_c in ferroelectric BaTiO₃ crystals.³² In this sense, it is not surprising that we observe $T_{SHG} > T_{max}$ even for the nominally stoichiometric sample. In addition, the nominally stoichiometric film [Fig. 3(b)] shows a discontinuous change in the slope of the SHG signal versus temperature as well as a large hysteresis effect. The sharp transition indicates that there is a critical onset of the ferroelectric transition that is not smeared by the presence of defects. The disappearance of the SHG signal at higher temperatures on heating can be explained by the greater correlation between polar nanoregions due to the reduced defect density. The pronounced SHG hysteresis indicates that the long-range polar order sets in more readily than in non-stoichiometric samples where it is gradual. Since no discontinuous jump is observed in the SHG signal of the nominally stoichiometric sample, the transition is still second order, but the T_c is well defined under heating and cooling, with a concomitant large hysteresis.

To characterize the soft mode, optical transmission measurements were made in the THz-frequency regime on two of the films (those with $x=0$ and $x=0.03$). The THz measurements were performed using a custom-made THz time-domain

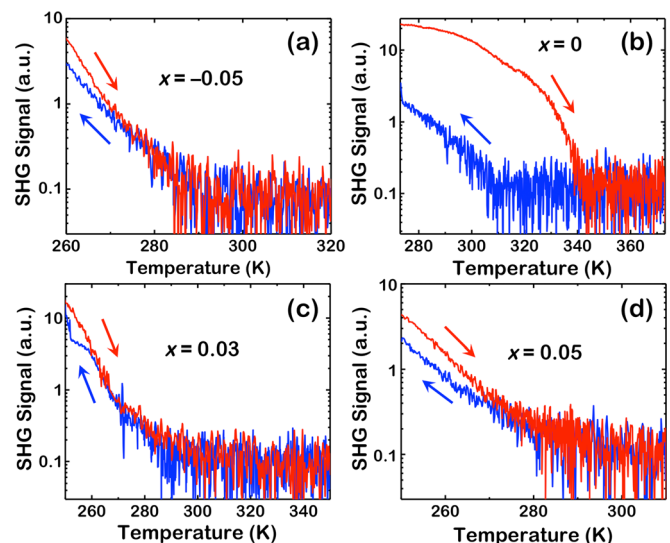


FIG. 3. SHG signal as a function of temperature of the Sr_{1+x}TiO_{3+ δ} films grown on (110) DyScO₃ substrates with (a) $x=-0.05$, (b) $x=0$, (c) $x=0.03$, and (d) $x=0.05$. Red arrows indicate the heating process. Blue arrows indicate the cooling process. All of the SHG signal measurements were performed at the same laser power intensity.

TABLE I. T_{\max} measured at 1 kHz from capacitance measurements and the onset temperature of the SHG signal (T_{SHG}) measured on cooling and heating.

$\text{Sr}_{1-x}\text{TiO}_{3+\delta}$	$x = -0.05$	$x = 0$	$x = 0.03$	$x = 0.05$
T_{\max} (1 kHz) [K]	281	283	261	231
T_{SHG} [K] (heating)	297	343	303	296
T_{SHG} [K] (cooling)	293	310	291	288

spectrometer.³³ The in-plane complex dielectric response of the thin films was calculated³⁶ from the complex transmittance spectra measured in an optical cryostat or in a furnace.

The real and imaginary parts of the in-plane dielectric constant (K_{11}) of the nominally stoichiometric film at several temperatures are shown in Fig. 4. The dominant feature in the spectra is due to the ferroelectric soft mode; its dramatic frequency variation with temperature is clearly seen. In addition, a central mode^{26,34,35} seems to contribute to the spectra near the low-frequency edge of the available data. Very similar behavior was reported for strained $\text{SrTiO}_3/\text{DyScO}_3$ films and multilayers grown by pulsed-laser deposition,^{36,37} and it was described by a model involving an oscillator (soft mode) coupled to a Debye relaxation (central mode)

$$K_{11}(\omega) = \frac{f(1-i\omega/\gamma) + g(\omega_{\text{SM}}^2 - \omega^2 - i\omega\Gamma) + 2\Delta\sqrt{fg}}{(\omega_{\text{SM}}^2 - \omega^2 - i\omega\Gamma)(1-i\omega/\gamma) - \Delta^2} + K_{11\infty}, \quad (1)$$

where ω_{SM} , Γ , and f are the soft mode eigenfrequency, damping, and oscillator strength, respectively; γ is the relaxation frequency; g is the relaxation strength, which acquires non-zero values only in the ferroelectric state; Δ is the coupling constant; and $K_{11\infty}$ is the contribution to the in-plane dielectric constant by higher frequency excitations. This model has been previously applied to a number of strained $\text{SrTiO}_3/\text{DyScO}_3$ thin film samples over a broad temperature range and for bias fields up to ~ 80 kV/cm.^{36,37} In that work,^{36,37} simultaneous fits of all spectra for all samples was performed (known f ; temperature independent γ and Δ).

The fitting parameters of the data in Fig. 4 were all found to acquire very similar values to those previously reported for strained SrTiO_3 films.^{36,37} Among these parameters, the soft mode frequency ω_{SM} was found to play a crucial role in the temperature evolution of the spectra. In particular, the temperature dependence of ω_{SM} in samples with $x=0$ and $x=0.03$ is well pronounced (see inset in Fig. 4). For the nominally stoichiometric film, ω_{SM} decreases (softens) down to much lower frequencies than for the non-stoichiometric film. Therefore, in the stoichiometric film, we can naturally expect the largest contribution of the soft mode to the permittivity. Indeed, this correlates well with the radio frequency (RF) results (Fig. 2) obtained on the same films. In addition, in the non-stoichiometric sample, the soft mode damping is larger; this can be caused by defects in the non-stoichiometric film as discussed above. According to the mode softening picture, the ferroelectric phase transition occurs in the temperature range 290–300 K in the nominally stoichiometric film and at 230–260 K in the sample with $x=0.03$; again, the same trend was observed in the RF data.

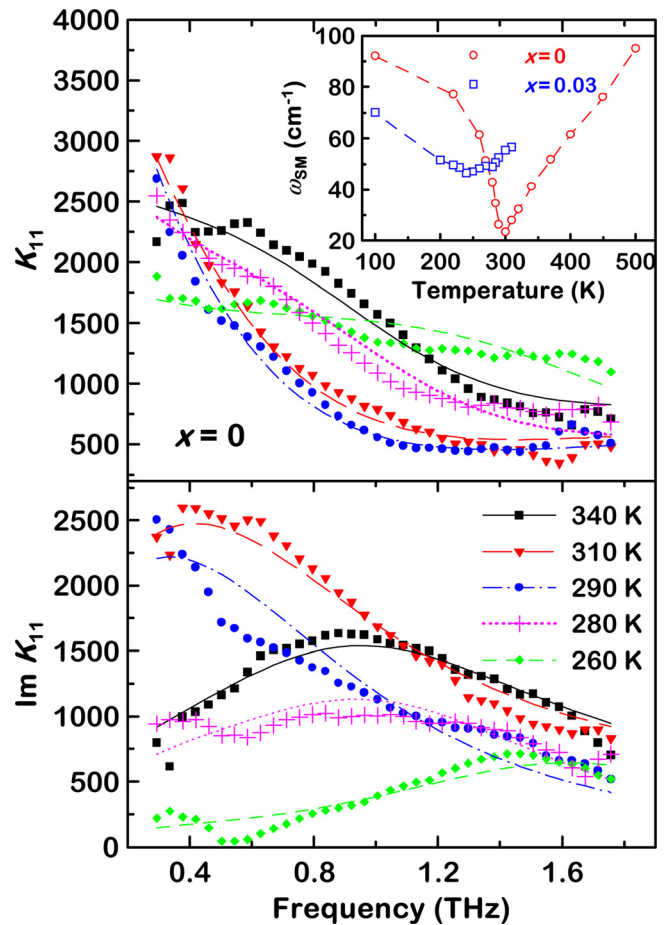


FIG. 4. Real and imaginary parts of the in-plane dielectric constant determined from optical transmission measurements of the nominally stoichiometric $\text{SrTiO}_3/\text{DyScO}_3$ film ($x=0$) at several temperatures. Symbols represent measured data; lines are fits by the model [Eq. (1)]. Inset: soft mode frequency behavior with temperature obtained from a fit to the samples with $x=0$ and $x=0.03$.

We see that in contrast to the relaxor behavior of non-stoichiometric samples, the nominally stoichiometric SrTiO_3 film undergoes a displacive phase transition with a slightly diffuse behavior in loss. In the context of Ref. 10, it is worth checking whether the diffusion of impurities from the underlying DyScO_3 substrate into the film could be responsible for the relaxor behavior. To test this possibility, the $x=0$ and $x=0.03$ samples (see Supplementary Fig. S3 of Ref. 13) were measured by secondary ion mass spectrometry (SIMS). The results reveal that comparable amounts of dysprosium (Dy) and scandium (Sc) diffused from the substrate into the films, i.e., the strength of random local electric fields arising from Sc'_{Ti} defects proposed in Ref. 10 should be comparable in these films. The origin of the different dielectrics (Fig. 2), SHG (Fig. 3), and soft-mode (Fig. 4) behavior can thus be solely attributed to the different Sr:Ti stoichiometry of these films.

Considering the difference of the soft mode temperature behavior in the nominally stoichiometric and non-stoichiometric sample, we can conclude that the nominally stoichiometric film shows classical features of a displacive ferroelectric. Small deviation from the stoichiometric formula is seen to result in a stiffened soft mode frequency and weaker temperature dependence. In other words, the soft mode frequency is a parameter that provides us with a rather

precise measure of the microscopic quality of the films. Nevertheless, it should be stressed that the soft mode contribution to the permittivity cannot completely account for the temperature dependence of the low-frequency dielectric constant. For the stoichiometric sample, the soft mode contribution to the in-plane dielectric constant at the phase transition is about 7000, i.e., one order of magnitude smaller than K_{11} obtained in the kHz–MHz frequency range. The central mode contribution always dominates near T_{\max} , so the phase transition is displacive with crossover to order-disorder type in the stoichiometric sample.

In conclusion, we have established the intrinsic dielectric properties of SrTiO₃ commensurately strained to (110) DyScO₃ using oxide MBE with meticulous control of the film composition. The smallest out-of-plane lattice constant, dispersion-free low-frequency permittivity, and a deep reduction of the soft mode frequency close to the ferroelectric transition were found in the nominally stoichiometric sample. We suggest that SrTiO₃ films should not show relaxor behavior as long as defect concentrations are reduced by precise composition control. Defects induced by a small error in the stoichiometry are likely responsible for the lack of repeatability in the dielectric behavior^{38,39} as well as transport properties of SrTiO₃ (Refs. 40 and 41) and for the inferior dielectric properties of thin films when compared to equivalent bulk crystals. This work highlights the sensitive coupling of the dielectric properties and electrical phenomena in oxide heterostructures with defects arising from non-stoichiometry.

The authors wish to thank P. Vaněk for his experimental help. The work at Cornell was supported by the ARO (Grant No. W911NF-09-1-0415). The work at Penn State was supported by the National Science Foundation through the MRSEC program (Grant No. DMR-0820404 and DMR-1210588). A portion of research was conducted at the Center for Nanophase Materials Sciences, which is sponsored at Oak Ridge National Laboratory by the Scientific User Facilities Division, Office of Basic Energy Sciences, U.S. Department of Energy. The work at Prague was supported by the Czech Science Foundation (projects 202/12/1163 and 202/09/H041) and Czech-American project LH13048.

¹K. A. Müller and H. Burkard, *Phys. Rev. B* **19**, 3593 (1979).

²W. Zhong and D. Vanderbilt, *Phys. Rev. B* **53**, 5047 (1996).

³J. G. Bednorz and K. A. Müller, *Phys. Rev. Lett.* **52**, 2289 (1984).

⁴C. Ang, Z. Yu, P. M. Vilarinho, and J. L. Baptista, *Phys. Rev. B* **57**, 7403 (1998).

⁵M. Itoh, R. Wang, Y. Inaguma, T. Yamaguchi, Y.-J. Shan, and T. Nakamura, *Phys. Rev. Lett.* **82**, 3540 (1999).

⁶J. H. Barrett, *Phys. Rev.* **86**, 118 (1952).

⁷E. Hegenbarth, *Phys. Status Solidi* **6**, 333 (1964).

⁸H. Uwe and T. Sakudo, *Phys. Rev. B* **13**, 271 (1976).

⁹J. H. Haeni, P. Irvin, W. Chang, R. Uecker, P. Reiche, Y. L. Li, S. Choudhury, W. Tian, M. E. Hawley, B. Craigo, A. K. Tagantsev, X. Q. Pan, S. K. Streiffer, L. Q. Chen, S. W. Kirchoefer, J. Levy, and D. G. Schlom, *Nature* **430**, 758 (2004).

¹⁰M. D. Biegalski, Y. Jia, D. G. Schlom, S. Trolier-McKinstry, S. K. Streiffer, V. Sherman, R. Uecker, and P. Reiche, *Appl. Phys. Lett.* **88**, 192907 (2006).

¹¹M. D. Biegalski, E. Vlahos, G. Sheng, Y. L. Li, M. Bernhagen, P. Reiche, R. Uecker, S. K. Streiffer, L. Q. Chen, V. Gopalan, D. G. Schlom, and S. Trolier-McKinstry, *Phys. Rev. B* **79**, 224117 (2009).

¹²H. W. Jang, A. Kumar, S. Denev, M. D. Biegalski, P. Maksymovych, C. W. Bark, C. T. Nelson, C. M. Folkman, S. H. Baek, N. Balke, C. M. Brooks, D. A. Tenne, D. G. Schlom, L. Q. Chen, X. Q. Pan, S. V. Kalinin, V. Gopalan, and C. B. Eom, *Phys. Rev. Lett.* **104**, 197601 (2010).

¹³See supplementary material at <http://dx.doi.org/10.1063/1.4793649> for additional details on film growth, *in situ* flux calibration, examination of in-plane lattice constant and crystalline quality by XRD, composition measurements by RBS, and interdiffusion analysis by SIMS.

¹⁴B. Velickov, V. Kahlenberg, R. Bertram, and M. Bernhagen, *Z. Kristallogr.* **222**, 466 (2007).

¹⁵Z. Yu, R. Droopad, and C. Overgaard, U.S. Patent No. 6,667,196 (23 December 2003).

¹⁶Z. Yu, Y. Liang, C. Overgaard, X. Hu, J. Curless, H. Li, Y. Wei, B. Craigo, D. Jordan, R. Droopad, J. Finder, K. Eisenbeiser, D. Marshall, K. Moore, J. Kulik, and P. Fejes, *Thin Solid Films* **462–463**, 51 (2004).

¹⁷P. Fisher, H. Du, M. Skowronski, P. A. Salvador, O. Maksimov, and X. Weng, *J. Appl. Phys.* **103**, 013519 (2008).

¹⁸A. Ichimiya and P. I. Cohen, *Reflection High-Energy Electron Diffraction* (Cambridge University Press, Cambridge, 2004).

¹⁹C. D. Theis and D. G. Schlom, *J. Vac. Sci. Technol. A* **14**, 2677 (1996).

²⁰J. B. Nelson and D. P. Riley, *Proc. Phys. Soc. London* **57**, 160 (1945).

²¹G. Rupprecht and W. H. Winter, *Phys. Rev.* **155**, 1019 (1967).

²²C. M. Brooks, L. Fitting Kourkoutis, T. Heeg, J. Schubert, D. A. Muller, and D. G. Schlom, *Appl. Phys. Lett.* **94**, 162905 (2009).

²³M. D. Biegalski, D. D. Fong, J. A. Eastman, P. H. Fuoss, S. K. Streiffer, T. Heeg, J. Schubert, W. Tian, C. T. Nelson, X. Q. Pan, M. E. Hawley, M. Bernhagen, P. Reiche, R. Uecker, S. Trolier-McKinstry, and D. G. Schlom, *J. Appl. Phys.* **104**, 114109 (2008).

²⁴N. J. Kidner, A. Meier, Z. J. Homrighaus, B. W. Wessels, T. O. Mason, and E. J. Garboczi, *Thin Solid Films* **515**, 4588 (2007).

²⁵Y. L. Li, S. Choudhury, J. H. Haeni, M. D. Biegalski, A. Vasudevarao, A. Sharan, H. Z. Ma, J. Levy, V. Gopalan, S. Trolier-McKinstry, D. G. Schlom, Q. X. Jia, and L. Q. Chen, *Phys. Rev. B* **73**, 184112 (2006).

²⁶A. S. Barker, Jr., *Phys. Rev. B* **12**, 4071 (1975).

²⁷R. J. D. Tilley, *J. Solid State Chem.* **21**, 293 (1977).

²⁸G. A. Samara, *J. Phys.: Condens. Matter* **15**, R367 (2003).

²⁹G. A. Samara and L. A. Boatner, *Phys. Rev. B* **61**, 3889 (2000).

³⁰C. Ang, Z. Yu, and Z. Jing, *Phys. Rev. B* **61**, 957 (2000).

³¹V. Bovtun, S. Veljko, S. Kamba, J. Petzelt, S. Vakhrušev, Y. Yakymenko, K. Brinkman, and N. Setter, *J. Eur. Ceram. Soc.* **26**, 2867 (2006).

³²E. Dul'kin, J. Petzelt, S. Kamba, E. Mojaev, and M. Roth, *Appl. Phys. Lett.* **97**, 032903 (2010).

³³P. Kužel, H. Němec, F. Kadlec, and C. Kadlec, *Opt. Express* **18**, 15338 (2010).

³⁴J. F. Scott, *Rev. Mod. Phys.* **46**, 83 (1974).

³⁵J. Petzelt, G. V. Kozlov, and A. A. Volkov, *Ferroelectrics* **73**, 101 (1987).

³⁶C. Kadlec, F. Kadlec, H. Němec, P. Kužel, J. Schubert, and G. Panaitov, *J. Phys.: Condens. Matter* **21**, 115902 (2009).

³⁷C. Kadlec, V. Skoromets, F. Kadlec, H. Němec, J. Schubert, G. Panaitov, and P. Kužel, *Phys. Rev. B* **80**, 174116 (2009).

³⁸T. Hirano, M. Taga, and T. Kobayashi, *Jpn. J. Appl. Phys., Part 2* **32**, L1760 (1993).

³⁹E. Breckenfeld, R. Wilson, J. Karthik, A. R. Damodaran, D. G. Cahill, and L. W. Martin, *Chem. Mater.* **24**, 331 (2012).

⁴⁰T. Ohnishi, K. Shibuya, T. Yamamoto, and M. Lippmaa, *J. Appl. Phys.* **103**, 103703 (2008).

⁴¹D.-W. Oh, J. Ravichandran, C.-W. Liang, W. Siemons, B. Jalan, C. M. Brooks, M. Huijben, D. G. Schlom, S. Stemmer, L. W. Martin, A. Majumdar, R. Ramesh, and D. G. Cahill, *Appl. Phys. Lett.* **98**, 221904 (2011).